Pseudoelasticity and the Strain-Memory Effect in an Ag-45 At. Pct Cd Alloy

R. V. KRISHNAN AND L. C. BROWN

A study has been made of pseudoelasticity and the strain-memory effect in β Ag-Cd alloys having a low temperature martensitic transformation. Tests on single crystals showed that maximum pseudoelasticity occurred in specimens with the tensile axis oriented close to $\langle 001 \rangle_\beta$ at temperatures 20° to 50°C above M_S. The habit plane for stress-induced martensite (SIM) was found experimentally to be $\sim(155)_\beta$ and agreed well with a value obtained from the phenomenological theory assuming a $(110)[1\bar{1}0]_\beta$ lattice-invariant shear. It is suggested that the macroscopic shear accompanying the transformation gives rise to the pseudoelastic strains, agreement with the experimental strain values being satisfactory. The strain-memory effect was explained as being due to a change from the $(011)[0\bar{1}1]_\beta$ lattice-invariant shear associated with thermal martensite to the $(110)[1\bar{1}0]_\beta$ shear associated with SIM.

THE effect of applied stress on martensitic transformations is well established.[1] The application of an uniaxial tensile stress can increase the transformation temperature, the change in this temperature being a function of the heat of transformation and the volume change associated with the change parent to martensite.[2] If the temperature is favorable, the martensite thus formed reverts to the parent phase on release of the stress giving rise to the well known pseudoelastic effect. This effect was first observed in Au-Cd alloys;[3] and indeed Au-Cd is probably the prototype system for nonferrous martensitic transformations. Considerable amounts of pseudoelastic strain have also been observed in In-Tl,[2] Cu-Al-Ni,[4,5] Cu-Zn-Sn,[6,7] and Cu-Zn-Si[6] alloys. The effect is more spectacular in single crystal specimens compared to polycrystalline ones.

Another effect related to stress-induced martensite (SIM) formation is the strain-memory effect in which a specimen that is deformed at low temperatures (below M_S) returns to its initial shape on heating above A_f. The strain-memory effect has been observed in Au-Cd,[8] In-Tl,[9] Ti-Ni,[10] Ti-Nb,[11] Cu-Zn-Sn,[7] Cu-Al-Ni,[5,12] and Cu-Zn[13] alloys. The deformation at low temperature results in a rearrangement of the martensitic plates, so as to accommodate the tensile strain. Almost all alloys which exhibit strain-memory effect have twinned martensitic structures. The reorientation, therefore, refers to the preferential growth of one twin orientation over the other.

The present investigation was undertaken to study SIM formation in Ag-45 at. pct Cd alloys. Both single and polycrystalline specimens were examined. Tensile tests were carried out over a wide temperature range and direct observation of the stress-induced martensite was made. The strain-memory effect was examined in single crystal specimens. A method was developed to calculate the amount of pseudoelastic strain that accompanies the transformation. The strain-memory effect is explained on the basis of a special choice of the lattice-invariant shear accompanying the transformation.

R. V. KRISHNAN is Research Assistant, Department Metaalkunde, Katholieke Universiteit, Leuven, Belgium. L. C. BROWN is Associate Professor, Department of Metallurgy, University of British Columbia, Vancouver, Canada. This paper is based upon a thesis submitted by R. V. KRISHNAN in partial fulfillment of the requirements of the degree of Doctor of Philosophy at the University of British Columbia.

Manuscript submitted March 3, 1972.

EXPERIMENTAL

Alloys were prepared by melting known weights of silver (99.95 pct) and cadmium (99.99 pct) in evacuated quartz tubes. These were subsequently homogenized at 680°C for 48 h. Polycrystalline specimens were made by hot rolling at 650°C to give strip 0.030 in. thick. Single crystal specimens were produced by a modified strain anneal method.[14] Strips 2 by 0.25 in. were cut from 0.045 in. thick rolled material using a jeweller's saw, and these were annealed and quenched to give the high temperature cubic structure. These specimens were then strained approximately 5 pct using an Instron tensile testing machine. Following this the specimen was slowly lowered into a molten salt bath held at 680°C at a rate of 10 cm/h, so that a crystal of the β phase was grown from one end of the specimen. The specimen was then quenched into iced caustic solution to retain the β phase single crystal. The surfaces were then mechanically polished to remove the contaminated layers and the gage section of the specimen was spark machined.

Tensile tests were generally carried out on an Instron machine at a cross-head speed of 0.005 in./min (corresponding to a strain rate of $\sim 1.4 \times 10^{-4}$ s^{-1}). Single crystal specimens were not normally taken to fracture but rather to a point where the whole gage length was completely martensitic. Polycrystalline specimens were taken to a strain of 5 pct before unloading. Chilled ethanol was used to vary the temperature of the specimens.

Electropolishing of the specimen was carried out using a 6 pct KCN solution. A stainless steel container was used as a cathode and a voltage of 2 V gave optimum results. This polishing gave a bright pink color to the retained β phase. Observations on the change in microstructure produced on deformation were made using a low power microscope equipped with a long-working-distance objective.

The habit plane of stress-induced martensite was

found by standard two surface analysis within an accuracy of ±3 deg, specimen orientations being determined by the Laue back-reflection technique.

The strain-memory effect was studied as follows: single crystal specimens were taken to a constant value of 5 pct strain at various temperatures and released. This gave the amount of elastic and pseudoelastic recovery. The specimen was then allowed to warm up to room temperature causing the reverse transformation to the β matrix. This resulted in a build-up of stress in the material which was later released. The strain associated with this was an approximate measure of the strain-memory effect.

RESULTS AND DISCUSSION

Single Crystal Specimens

The Ag-45 at. pct Cd alloy used had the following transformation temperatures: M_S = –74°C, M_f = –98°C, A_S = –80°C, and A_f = –67°C.

EFFECT OF TEMPERATURE

Fig. 1 shows a series of tensile curves at different temperatures for a specimen whose axis is close to the [001]* corner of the unit triangle. At temperatures (–90°C) below M_S, the specimen is partially or fully martensitic to start with, and application of external stress causes both formation of new martensite and deformation of existing martensite. The martensite is stable and the specimen shows very little recovery on unloading.

*All indices are given with respect to the parent cubic phase unless indicated otherwise.

At temperatures above M_S, the stress-strain curve is initially linear up to a stress level at which stress-induced martensite forms. SIM forms in bursts at lower temperatures (–60° and –55°C) but forms more gradually at higher temperatures as is revealed by the absence of serrations in the transformation portion of the curve (-45° and –10°C).

The martensite formation in these cases is more of the thermoelastic type considering the fact that there is virtually no hysteresis associated with the transformation.

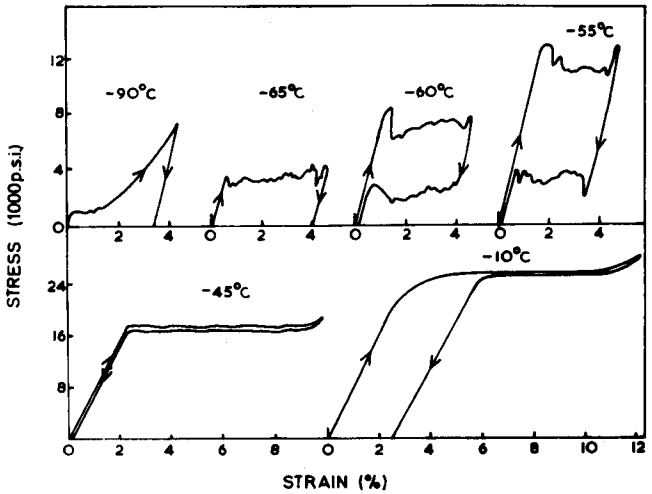

Fig. 1—Stress-strain curves (over a series of temperatures) for a specimen whose tensile axis is oriented close to [001].

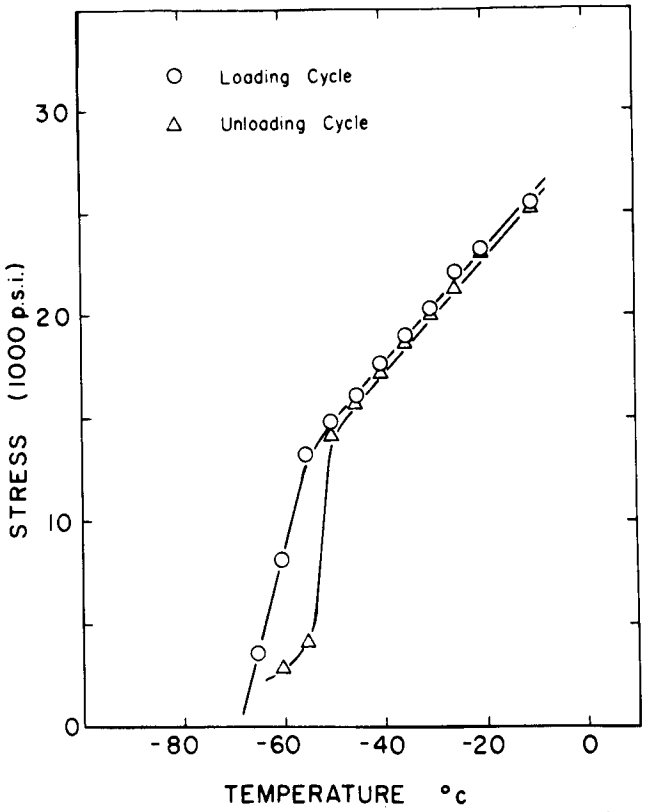

Fig. 2—Variation of the stress necessary to form SIM with temperature for a specimen oriented close to [001].

Upon unloading, the martensite thus formed remains stable or disappears depending upon the temperature of the test. The martensite is unstable at temperatures above A_f, and therefore, should disappear completely on unloading (see –60°C, –55°C, –45°C). If the temperature is below A_S, then martensite should remain stable (*e.g.* at –90°C). In fact the test at –65°C shows nonreversible martensite, perhaps indicating that stressing the specimen hinders the reversion of martensite to the β matrix. Fig. 2 shows a plot of the stress needed to form SIM as a function of temperature. It also includes the stress level corresponding to the point when the last trace of martensite disappears on unloading. The stress necessary to form the martensite varies linearly with temperature, exhibiting a two-stage behavior. The transition from one region to the other corresponds to the change in the nature of formation of martensite. The stress necessary to form martensite is by definition zero at the M_S temperature. The initial portion of the curve must, therefore, extrapolate to the M_S temperature at zero stress. The extrapolated value is –70°C compared to the experimentally determined value of –74°C.

At higher temperatures, –10°C in Fig. 1, the stress necessary to form martensite exceeds the yield stress of the material. At this stage the material deforms plastically initially until a point is reached when the material is sufficiently work hardened to support the stress needed to form martensite at that temperature. The martensite thus formed is reversible, as it is well above the A_f temperature. If, however, the specimen is tested at this temperature again, then martensite will form from the start without any plastic deformation having to precede it.

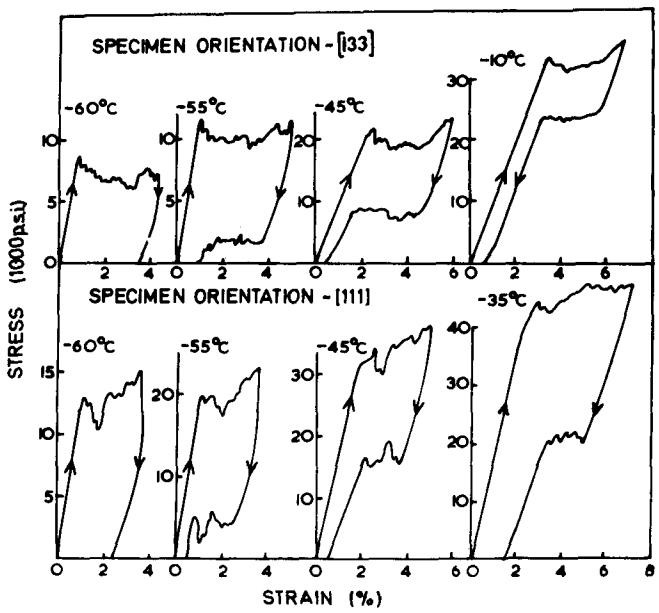

Fig. 3—Stress-strain curves at different temperatures for specimens with the tensile axis oriented close to [133] and [111].

EFFECT OF ORIENTATION

Stress-strain curves at different temperatures are shown in Figs. 1 and 3 for single crystal specimens with three separate orientations of the tensile axis—close to [001], Fig. 1, close to [133], and [111], Fig. 3.

At –60°C, all specimens exhibit a serrated stress-strain curve, indicating that martensite was formed in bursts. The [001] orientation shows full recovery, whilst the other specimens do not show any recovery other than the true elastic recovery.

At –55°C, the martensitic formation is still of the burst type, but now is recovered in all three specimens (–55°C is well above the A_f temperature for the alloy, –67°C). The recovery is close to 100 pct for the [001] orientation, whereas for the other two orientations it is 90 pct.

At –45°C, the [001] specimen transforms at a constant load giving a significantly higher strain corresponding to complete transformation to martensite. The other two specimens still show serrated stress-strain curves. Again recovery is complete for the [001] orientation, but only ~95 pct for [133] and ~85 pct for [111].

At –35°C, the [001] and [133] specimens behave as before, but the [111] orientation gives a considerable amount of permanent set after unloading with only 75 pct recovery. No further higher temperature tests were carried out on this specimen.

At –10°C, the [001] specimen initially deforms plastically, before the transformation takes over. The reversal of martensite is complete, but the initial plastic deformation gives a permanent set to the specimen. The [133] specimen transforms on application of stress and recovers almost 95 pct. However, the amount of strain given to cause complete transformation to martensite is small.

The amount of pseudoelasticity obtained is least for the specimen whose axis is close to [111] and also there is less tendency for complete recovery in this case. The specimen whose axis is close to [001] can be extended ~9 pct without having any permanent set. This orientation shows the clearest transition between the serrated stress-strain curve and the smooth high temperature curve.

Polycrystalline Specimens

Polycrystalline specimens were tested over the complete range of temperatures. Fig. 4 shows representative tensile curves at different temperatures and Fig. 5 shows the values of the stress at which the curves deviated from linearity. Fig. 5 can be divided into three different regions, depending on the temperature relative to M_S.

REGION b

This region covers the temperature range from –75° to –20°C, *i.e.* from M_S to 47°C above A_f. On loading the specimen in this temperature region, the matrix deforms elastically up to a certain value of the stress, which is a function of the temperature, and above this stress transforms to martensite.* The stress needed for the formation of martensite increases with increase in the temperature of testing, as expected.

*The formation of SIM could easily be detected because of the accompanying color change in the specimen, from pink to silver.

REGION a: ($T < M_S$)

In this region, the specimen is partly or fully martensitic to start with. The increase in the applied stress causes reorientation and deformation of the existing martensitic plates and also the formation of SIM. The formation of SIM is completed at M_f(–98°C)

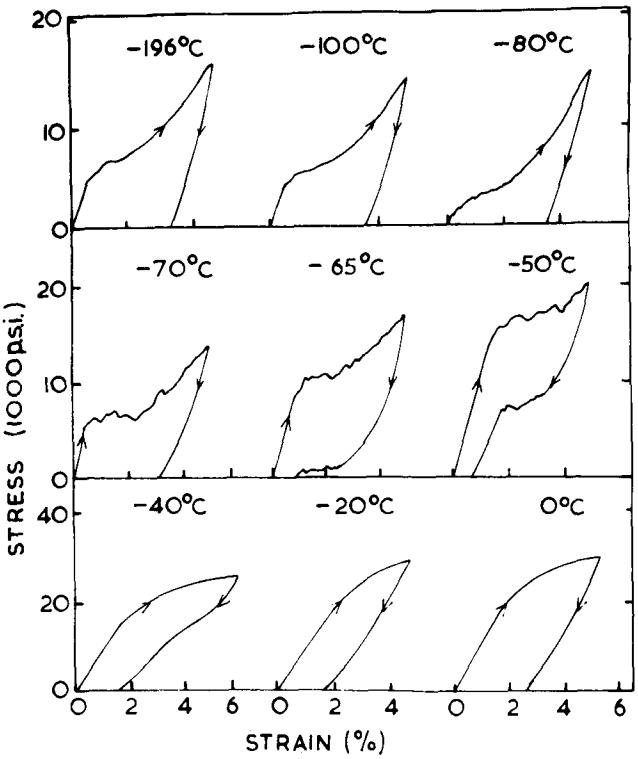

Fig. 4—Stress-strain curves for polycrystalline specimens over a series of temperatures.

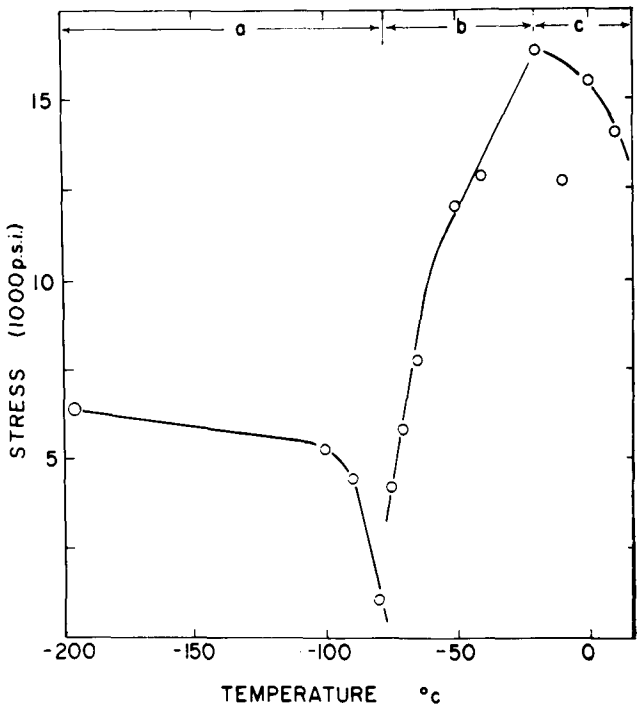

Fig. 5—Stress level corresponding to the initial deviation from linearity in the tensile curves of Fig. 4 plotted as a function of temperature for polycrystalline specimens.

and below this there is only a reorientation of the existing thermal martensite.

REGION c

For temperatures more than 50°C above A_f, the transformation stress is so high that plastic deformation of the specimen occurs first. The stress corresponding to the point of deviation in the tensile curves then equals the yield stress of the material at that temperature. The drop in the yield stress with temperature is in keeping with the behavior of bcc materials. Even though the material deforms plastically in the initial stages, it is possible that the specimen will ultimately transform to martensite provided the stress level is high enough to cause the transformation, (compare this with Fig. 1 at –10°C).

The martensite thus formed reverts back to the β phase upon unloading if the test temperature is above A_s. The reversion is nearly complete in the case where the test temperature is above A_f and is only partial in the temperature range A_s to A_f.

The maximum recovery obtained was always less than 100 pct, unlike single crystals, and this is believed to be due to the plastic deformation occurring along the grain boundaries.

Strain-Memory Effect

Fig. 6 shows the strain-memory recovery plotted as a function of temperature for specimens strained approximately 5 pct. The amount of pseudoelasticity observed is also included. Eisenwasser and Brown[7] showed that the strain-memory effect and pseudoelasticity were complementary in nature and the relative amounts depended on the temperature of the test. The present work shows a similar effect. At low temperatures there is relatively little pseudoelasticity and most of the recovery is by the strain-memory effect. The strain-memory effect drops drastically above A_f and at the same time there is a significant increase in pseudoelasticity from approximately 15 to 97 pct. The total recovery, however, is always close to 100 pct.

The changes that take place in the microstructure of the specimen when deformed at a temperature below M_f are shown in Fig. 7. The change in the disposition of the martensite plates is clearly revealed. Whether there is a change in the structure of the martensite associated with this reorientation is not known, since it was not practical to obtain single crystal diffraction patterns at low temperatures.

Habit Planes of SIM

Thermal martensite in Ag-45 at. pct Cd alloys has an orthorhombic crystal structure.[15] Electron microscopy of these alloys has proved complicated because of the spontaneous transformation to martensite similar to the one reported by Hull.[16] In the case of Ag-Cd alloys a twinned fcc structure has been observed in some thin foils at room temperature.[17,18] However, this is not the structure of the low temperature martensite, which consists of a faulted structure.[15] The habit plane normal was calculated using the analysis of Wechsler and Otte,[19] a modification of the basic W-L-R theory[20] for a generalized lattice-invariant shear system. A lattice correspondence of $[100]_C \parallel [110]_0$ and $(001)_C \parallel (001)_0$ (Group II correspondence in Ref. 19) was assumed.

The lattice parameters used in the calculations were a = 3.314Å for the cubic phase and a = 3.0968Å, b = 4.8651Å and c = 4.7536Å for the orthorhombic martensite phase.[15] The probable error in the lattice parameters is estimated to be no more than ±0.010Å.

Two calculations for the habit plane were carried

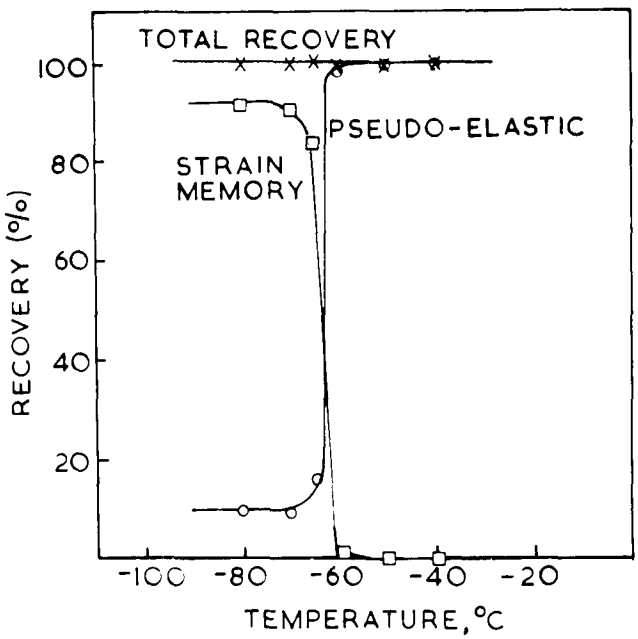

Fig. 6—Strain-memory and pseudoelastic recovery vs temperature for a single crystal specimen. The total recovery (strain-memory + pseudoelastic) is indicated as x.

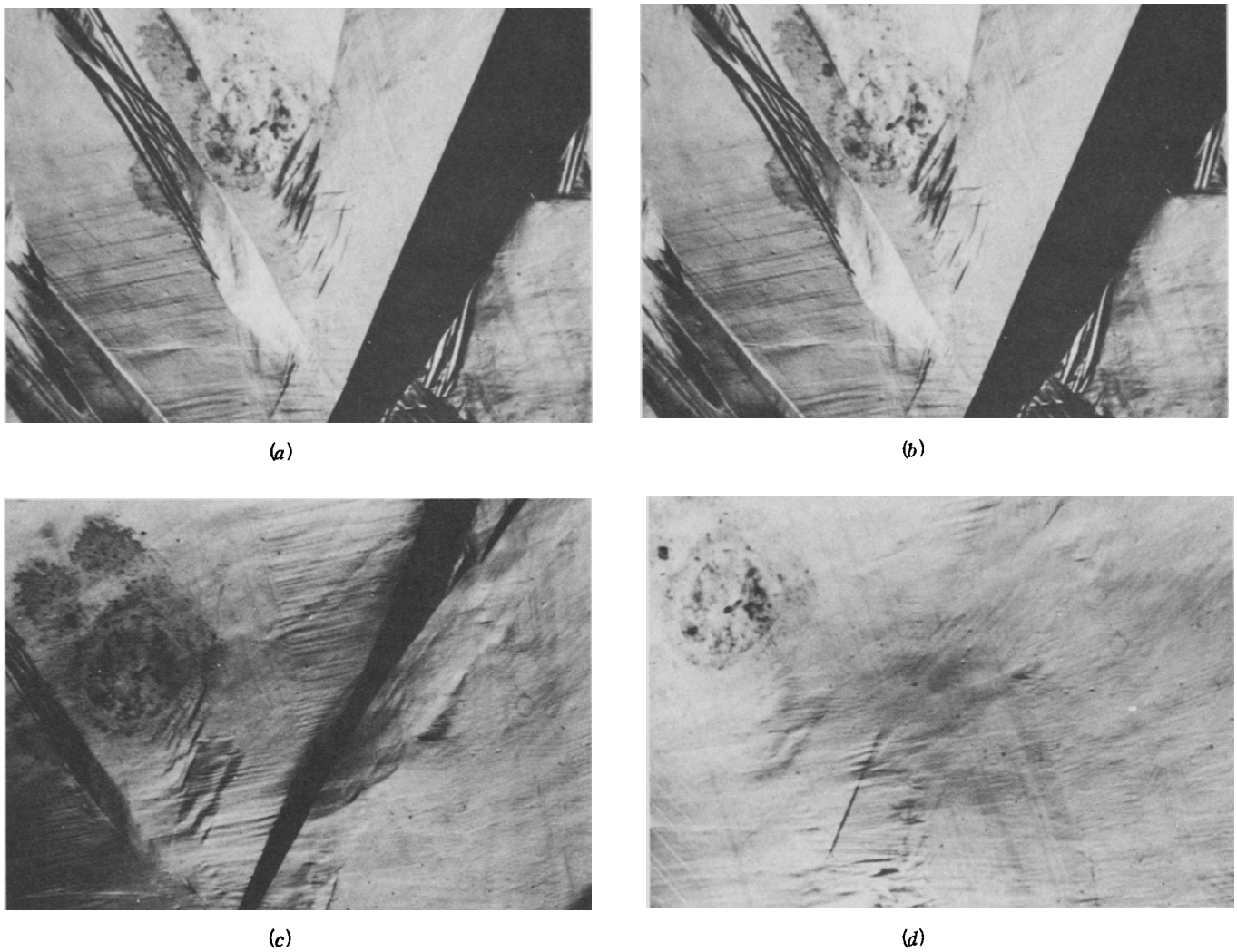

Fig. 7—Changes in the microstructure of thermal martensite on deforming below M_f. Magnification 60 times. (*a*) → (*d*) show changes as the external stress is increased gradually.

through, one using the actual values for the lattice parameters and one assuming a dilation, δ, of 1.0055 so as to give zero volume change on transformation. This latter concept leads to the total macroscopic distortion being in the form of simple shear, which simplifies further calculations. As shown in Fig. 8 the experimental habit planes for thermal martensite lie intermediate between the two calculated values if a $(011)[0\bar{1}1]$ lattice-invariant shear is assumed, corresponding to the stacking fault shear observed by electron microscopy.

In SIM, the habit plane normals show some scatter, but cluster around [155] as shown in Fig. 8 and so definitely have a different habit plane from thermal martensite. If it is considered that SIM has the same crystal structure as thermal martensite, then the observed habit plane can be explained assuming a lattice invariant shear of $(110)[1\bar{1}0]$, another variant of the stacking fault shear. Other possible lattice-invariant shears such as $\{011\}\langle 31\bar{1}\rangle$ and $\{112\}\langle 11\bar{1}\rangle$ do not give habit plane normals close to the experimental values. The crystallographic parameters calculated from the theory are given in Table I.

From Table I it is clear that the amount of macroscopic shear accompanying thermal martensite formation is less than that associated with SIM. Therefore, it is concluded that in the absence of external stress, a minimum value of the macroscopic shear governs the choice of particular lattice-invariant shear selected.

The formation of SIM is accompanied by an increase in length of the specimen in the direction of the applied stress. The macroscopic shear associated with the transformation may be considered responsible for this length increase. Fig. 9 gives the geometrical construction involved, region *ABCD* transforming to martensite with macroscopic shear $\tan\gamma = EB/OB$ and a corresponding length change *BG*. Obviously the larger the macroscopic shear the greater the length increase. This is the reason for the selection of the $(110)[1\bar{1}0]$ variant of the lattice-invariant shear for SIM, since it will give a larger length increase.

In general only one orientation of the habit plane occurs in SIM, in contrast to the large number of orientations in thermal martensite. The variant that is selected is the one for which the applied stress provides the greatest assistance to martensite formation. This is characterized by the resolved shear stress being a maximum in the direction of the macroscopic shear for that variant. The resolved shear stress is given by $\cos\phi\cos\lambda$ where ϕ is the angle between the tensile axis and the habit plane normal and λ is the angle between the tensile axis and the macroscopic shear di-

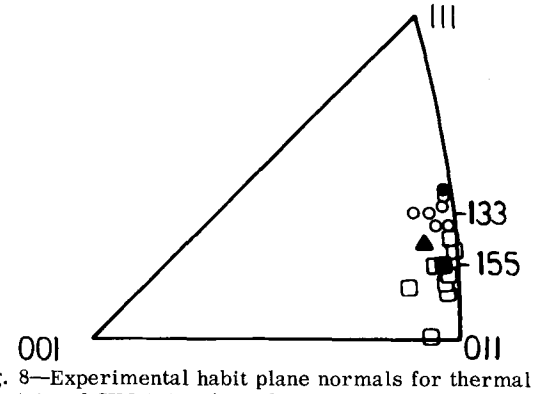

Fig. 8—Experimental habit plane normals for thermal martensite (○) and SIM (□). (▲) and (●) are calculated values of the same in the case of thermal martensite for $\delta = 1.0$ and $' = 1.0055$. (■) is in the case of SIM calculated for $\delta = 1.0055$.

rection. In Table II observed values of the angle ϕ are given for various orientations of the tensile axis, and are compared with the calculated values for the possible variants in each case. In fact the procedure employed is to select a particular variant of the habit plane normal $[n_1\, n_2\, n_3]$ and the corresponding macroscopic shear $[d_1\, d_2 - d_3]$ and then to determine the values of ϕ and $\cos\phi\cos\lambda$ for various possibilities of the tensile axis (*e.g.* [911], [9$\bar{1}$1], [91$\bar{1}$], [9$\bar{1}\bar{1}$]) that would result in a positive linear strain. Table II shows clearly that the observed habit planes do indeed have near maximum values for the resolved shear stress. The second variant of the habit plane normal $[n_1\, n_2 - n_3]$ and the corresponding shear direction $[d_1\, d_2\, d_3]$ are crystallographically equivalent to the first variant in SIM and will result in a preferred tensile axis of the form $[hk-l]$. However, the value of ϕ remains unaltered. It is interesting to note that if one considers the resolved shear stress on the lattice-invariant shear system viz. (110) [1$\bar{1}$0] the different orientations of the tensile axis give the same value and therefore this does not provide a criterion for the selection of any particular orientation of the tensile axis.

From Fig. 9 it can be shown that the strain associated with the formation of a martensite plate is $\frac{1}{2}\sin 2\phi\tan\gamma$. However, this is not the general solution since it is assumed that the tensile axis, habit plane normal and the macroscopic shear direction are coplanar. In the general case the linear strain equals $\frac{1}{2}\sin 2\phi\tan\gamma\cos\alpha$ where α is the angle between the plane of tension (plane containing the tensile axis and the habit plane normal) and the plane of shear* (plane defined by the habit plane normal and the macroscopic shear direction).

*The plane of shear is different from the shear plane, which in this case is the habit plane and remains invariant.

Fig. 10 shows the various planes and angles involved in the construction. For a given habit plane normal $\underline{n}$, the tensile axis, $\underline{p}$, must lie within the two great circles N and P for positive elongations to be obtained.

Calculations were made for a large number of orientations of the tensile axis $\langle hkl\rangle$ with a (155) habit plane to determine the most favorable variant of the tensile axis and the corresponding elongation. The results are plotted in Fig. 11 which shows contour lines joining orientations of the tensile axis which give the same value of linear strain. The elongation is greatest for orientations close to [001] and decreases progressively on moving away from this. Very limited elastic strains are possible for orientations close to [111] and it is clear that any larger strain is taken up plastically and is nonreversible.

The amounts of strain obtained experimentally are in good agreement with the theory. The specimens shown in Figs. 1 and 3 were stressed until they had completely transformed to martensite, so that the length of the plateau corresponds to the strain associated with the martensite transformation. Subtracting any permanent set from this gives very approximately the experimental pseudoelasticity. Results at –45°C where all the specimens had maximum elasticity gave pseudoelastic strains of 6 pct, $3\frac{1}{2}$ pct, and $2\frac{1}{2}$ pct for specimens oriented close to [001], [133], and [111],

Table I. Crystallographic Parameters Calculated From the Theory for $\delta = 1.0055$

	Thermal Martensite	Stress-Induced Martensite
Lattice-invariant shear system	(011)[0$\bar{1}$1]	(110)[1$\bar{1}$0]
Amount of lattice-invariant shear g	0.054	0.059
Habit plane normal $\underline{n}$	0.6723	0.7136
	0.2822	0.1482
	0.6844	0.6847
Macroscopic shear direction	0.6533	0.6704
	0.2092	0.1392
	–0.7276	–0.7288
Amount of macroscopic shear	0.071	0.125

Table II. Comparison Between the Observed and Calculated Values of ϕ (Angle Between the Habit Plane Normal and the Tensile Axis)

Tensile Axis	ϕ Observed, deg	Possible Variants of Tensile Axis	ϕ Calculated, deg	$\cos\phi\cos\lambda$
<911>	42	911	37.2	0.476
		9$\bar{1}$1	40.2	0.433
	40	91$\bar{1}$	49.8	0.489
		9$\bar{1}\bar{1}$	52.2	0.446
<511>	55	511	32.1	0.450
		5$\bar{1}$1	37.8	0.378
		51$\bar{1}$	54.3	0.473
		5$\bar{1}\bar{1}$	58.2	0.399
<13, 7, 5>	62	13, 7, 5	28.2	0.341
		13, $\bar{7}$, 5	41.6	0.195
		13, 7, $\bar{5}$	63.8	0.377
		13, $\bar{7}$, $\bar{5}$	72.0	0.225
<6, 5, 2>	69	6, 5, 2	37.5	0.320
		6, $\bar{5}$, 2	52.5	0.141
		6, 5, $\bar{2}$	63.1	0.347
		6, $\bar{5}$, $\bar{2}$	74.4	0.159
<16, 10, 5>	65	16, 10, 5	33.3	0.363
		16, $\bar{1}$0, 5	46.8	0.199
		16, 10, $\bar{5}$	61.0	0.391
		16, $\bar{1}$0, $\bar{5}$	70.5	0.222

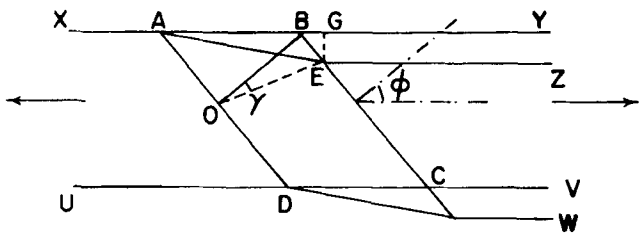

Fig. 9—Geometrical construction to calculate the tensile strain involved in the transformation.

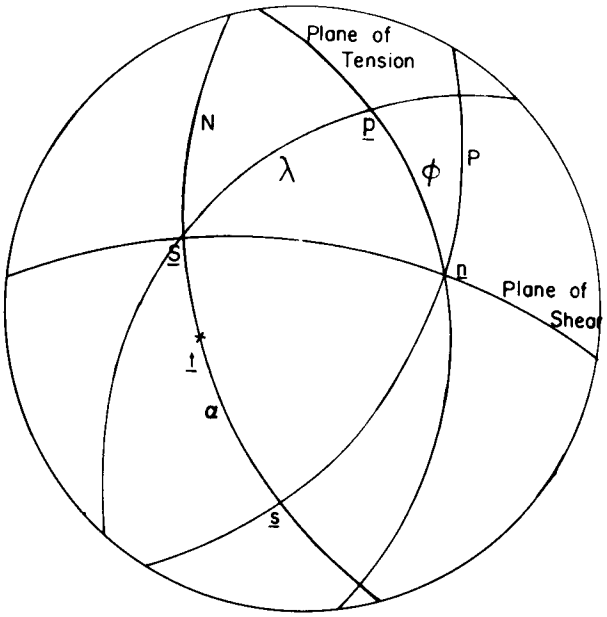

n : Habit Plane Normal.

p : Tensile Axis.

s : Normal to Plane of Shear.

t : Normal to Plane of Tension.

S : Macroscopic Shear Direction.

$\phi = \Lambda\, \underline{n}\,\underline{p} \qquad \lambda = \Lambda\, \underline{S}\,\underline{p} \qquad \alpha = \Lambda\, \underline{t}\,\underline{s}$

Fig. 10—Stereographic projection showing the various angular relationships involved in the calculation.

respectively. The corresponding theoretical strains are 6.3 pct, 3 pct, and 1.9 pct for the three orientations in agreement with the experimental values. Note that the total elastic strains in the specimens are considerably greater owing to the large amount of elastic strain prior to the martensitic transformation. This is due to the low resistance of the β matrix to $\{011\}\langle 011\rangle$ shear and has been discussed by Eisenwasser and Brown.[7]

A calculation similar to the one above can also be carried through for the case of thermal martensite. However the maximum strain possible is $\frac{1}{2}\tan\gamma$ (for the case when $\phi = 45$ deg and $\alpha = 0$ deg); therefore, even if thermal martensite were to form in an oriented manner, the maximum possible strain would be ~3.5 pct. Hence, it is suggested that on stressing the thermal martensite, a change to SIM takes place, with the SIM forming in such an orientation as to give the required specimen elongation. The change in the microstructure shown in Fig. 7 supports this view. The amounts of strain associated with this structure change will be similar to the strains calculated for the case of pseudoelasticity.

CONCLUSIONS

1) Pseudoelasticity occurs in both single and polycrystalline Ag-45 at. pct Cd alloys on deformation at temperatures above A_f. At lower temperatures the strain-memory effect is observed.

2) Pseudoelasticity is greatest for orientations of the tensile axis close to [001] and least for orientations close to [111].

3) The habit plane for SIM is close to (155), different

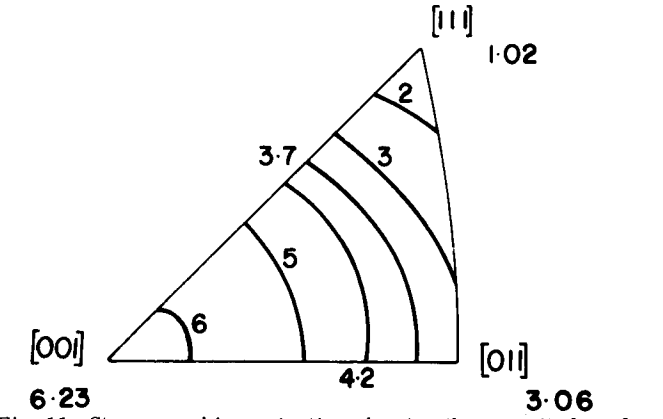

Fig. 11—Stereographic projection showing the magnitudes of strain associated with the formation of SIM for various orientations of the tensile axis.

from the (133) orientation found for thermal martensite. The habit plane calculated from the phenomenological theory assuming a $(110)[1\bar{1}0]$ lattice-invariant shear is in good agreement with experiment.

4) The macroscopic shear associated with the formation of SIM appears to be responsible for the large pseudoelastic strains observed. These are calculated to be 6, 3, and 2 pct for orientations of the tensile axis of [001], [133], and [111], respectively, in moderate agreement with experiment.

5) At temperatures above M_f, the strain-memory effect is due at least partly to the formation of SIM which is stable on removal of the stress. Thermal martensite also shows a strain-memory effect and this appears to be due to a change from thermal martensite with a $(011)[0\bar{1}1]$ lattice-invariant shear to SIM with a $(110)[1\bar{1}0]$ lattice-invariant shear.

ACKNOWLEDGMENTS

The authors wish to thank Drs. E. B. Hawbolt and D. Tromans for helpful discussions. Financial assistance provided by the National Research Council of Canada under Grant A-2549 and that awarded in the form of a graduate fellowship to one of the authors (RVK) are gratefully acknowledged.

REFERENCES

1. J. C. Patel and M. Cohen: *Acta Met.*, 1953, vol. 1, p. 531.
2. M. W. Burkart and T. A. Read: *J. Metals*, November 1953, p. 1516.
3. J. Intrater, L. C. Chang, and T. A. Read: *Phys. Rev.*, 1952, vol. 86, p. 598.
4. W. A. Rachinger: *J. Aust. Inst. Metals*, 1960, vol. 5, p. 114.
5. K. Oishi and L. C. Brown: *Met. Trans.*, 1971, vol. 2, p. 1971.
6. H. Pops: *Met. Trans.*, 1970, vol. 1, p. 251.
7. J. D. Eisenwasser and L. C. Brown: *Met. Trans.*, 1972, vol. 3, p. 1359.
8. D. S. Lieberman, T. A. Read, and L. C. Chang: *Phys. Rev.*, 1951, vol. 82, p. 340.
9. Z. S. Basinski and J. W. Christian: *Acta Met.*, 1954, vol. 2, p. 148.
10. R. G. deLange and J. A. Zijderveld: *J. Appl. Phys.*, 1968, vol. 39, p. 2195.
11. C. Baker: *Metal Sci. J.*, 1971, vol. 5, p. 92.
12. K. Otsuka and K. Shimizu: *Scripta Met.*, 1970, vol. 4, p. 469.
13. C. M. Wayman: *Scripta Met.*, 1971, vol. 5, p. 489.
14. E. Hornbogen, A. Segmüller, and G. Wasserman: *Z. Metallk.*, 1957, vol. 48, p. 379.
15. R. V. Krishnan and L. C. Brown: *Met. Trans.*, 1973, vol. 4, in press.
16. D. Hull: *Phil. Mag.*, 1962, vol. 7, p. 537.
17. R. V. Krishnan: Ph.D. Thesis, Department of Metallurgy, University of British Columbia, July 1971.
18. A. Nagasawa: *J. Phys. Soc. Japan*, 1972, vol. 32, p. 864.
19. M. S. Wechsler and H. M. Otte: *Acta Met.*, 1961, vol. 9, p. 117.
20. D. S. Lieberman, M. S. Wechsler, and T. A. Read: *J. Appl. Phys.*, 1955, vol. 26, p. 473.